AMERICAN SOCIETY FOR MICROBIOLOGY | Journal of Bacteriology®

RESEARCH ARTICLE

TetR Family Transcriptional Regulator PccD Negatively Controls Propionyl Coenzyme A Assimilation in *Saccharopolyspora erythraea*

Zhen Xu,[a] Miaomiao Wang,[a] Bang-Ce Ye[a,b]

Lab of Biosystems and Microanalysis, State Key Laboratory of Bioreactor Engineering, East China University of Science and Technology, Shanghai, China[a]; School of Chemistry and Chemical Engineering, Shihezi University, Xinjiang, China[b]

ABSTRACT Propanol stimulates erythromycin biosynthesis by increasing the supply of propionyl coenzyme A (propionyl-CoA), a starter unit of erythromycin production in *Saccharopolyspora erythraea*. Propionyl-CoA is assimilated via propionyl-CoA carboxylase to methylmalonyl-CoA, an extender unit of erythromycin. We found that the addition of *n*-propanol or propionate caused a 4- to 16-fold increase in the transcriptional levels of the SACE_3398–3400 locus encoding propionyl-CoA carboxylase, a key enzyme in propionate metabolism. The regulator PccD was proved to be directly involved in the transcription regulation of the SACE_3398–3400 locus by EMSA and DNase I footprint analysis. The transcriptional levels of SACE_3398–3400 were upregulated 15- to 37-fold in the *pccD* gene deletion strain (Δ*pccD*) and downregulated 3-fold in the *pccD* overexpression strain (WT/pIB-*pccD*), indicating that PccD was a negative transcriptional regulator of SACE_3398–3400. The Δ*pccD* strain has a higher growth rate than that of the wild-type strain (WT) on Evans medium with propionate as the sole carbon source, whereas the growth of the WT/pIB-*pccD* strain was repressed. As a possible metabolite of propionate metabolism, methylmalonic acid was identified as an effector molecule of PccD and repressed its regulatory activity. A higher level of erythromycin in the Δ*pccD* strain was observed compared with that in the wild-type strain. Our study reveals a regulatory mechanism in propionate metabolism and suggests new possibilities for designing metabolic engineering to increase erythromycin yield.

IMPORTANCE Our work has identified the novel regulator PccD that controls the expression of the gene for propionyl-CoA carboxylase, a key enzyme in propionyl-CoA assimilation in *S. erythraea*. PccD represses the generation of methylmalonyl-CoA through carboxylation of propionyl-CoA and reveals an effect on biosynthesis of erythromycin. This finding provides novel insight into propionyl-CoA assimilation, and extends our understanding of the regulatory mechanisms underlying the biosynthesis of erythromycin.

KEYWORDS propionate metabolism, propionyl-CoA assimilation, erythromycin biosynthesis, transcriptional regulation

Saccharopolyspora erythraea, a Gram-positive filamentous soil bacterium, is used for production of the antibiotic erythromycin. Erythromycin and its derivatives play a vital role in medicine, with annual sales reaching several billion dollars annually (1). Historically, multiple rounds of random mutagenesis and selection have been used to obtain overproducing mutants for industrial production. Nowadays, genetic engineering of the pathways involved in biosynthesis of secondary metabolites also holds promises to enhance production (2–4).

Received 20 April 2017 **Accepted** 20 July 2017

Accepted manuscript posted online 31 July 2017

Citation Xu Z, Wang M, Ye B-C. 2017. TetR family transcriptional regulator PccD negatively controls propionyl coenzyme A assimilation in *Saccharopolyspora erythraea*. J Bacteriol 199:e00281-17. https://doi.org/10.1128/JB.00281-17.

Editor Tina M. Henkin, Ohio State University

Address correspondence to Bang-Ce Ye, bcye@ecust.edu.cn.

Production of one unit of erythromycin requires one propionyl coenzyme A (propionyl-CoA) to provide a starter unit and six (2*S*)-methylmalonyl–CoAs to provide extender units to form 6-deoxyerythronolide B (6-dEB) (5). The experiments of Reeves et al. indicated that methylmalonyl-CoA was a limiting factor for erythromycin biosynthesis (6). Engineering of the methylmalonyl-CoA metabolic flux of *S. erythraea* through knockout of the methylmalonyl-CoA mutase operon resulted in a 50% increase in erythromycin production in an oil-based fermentation medium (7). Integrating genomics, transcriptomics, and proteomics comparisons between the wild-type strain and the industrial highly producing strain of *S. erythraea* revealed that the industrial strain has a high flux of metabolites toward erythromycin biosynthesis and degradation pathway of branched-chain amino acids (8). Because branched-chain amino acids are a source of methylmalonyl-CoA, the significantly higher expression levels of *ilvB* (acetolactate synthase large subunit gene, SACE_4565), *acd* (acyl-CoA dehydrogenase gene, SACE_4125 and SACE_5025), and *mmsA* (methylmalonate-semialdehyde dehydrogenase gene, SACE_4672) in the highly producing strain may lead to an increased supply of propionyl-CoA and methylmalonyl-CoA, key precursors for erythromycin synthesis. This is also supported by an increased erythromycin yield when different genes of the branched-chain amino acid metabolism were overexpressed (9). The quantitative analysis of metabolic carbon flux indicated that a high consumption rate of propanol increased propionyl-CoA and methylmalonyl-CoA concentrations. The addition of *n*-propanol at a concentration of 1% (vol/vol) increased erythromycin production by 20% (10). Analysis of *n*-[^{18}O]propanol metabolic carbon flux suggested that the oxygen atoms of 6-dEB are largely derived from *n*-propanol (11). Propanol is converted into propionate, which is subsequently metabolized to propionyl-phosphate or propionyl-CoA by propionate kinase or acetyl/propionyl-CoA synthetase. However, propionyl-CoA is an inhibitor of CoA-dependent enzymes such as pyruvate dehydrogenase, succinyl-CoA synthetase, and ATP citrate lyase (12–16). Therefore, the assimilation of propionyl-CoA needs to be precisely regulated to prevent its accumulation within the cell.

In most microorganisms, so far, two pathways were found for propionyl-CoA assimilation: the methylcitrate cycle (MCC) that converts propionyl-CoA to pyruvate and the propionyl-CoA carboxylase (PCC) pathway, which is responsible for the metabolism of propionyl-CoA to methylmalonyl-CoA. No gene encoding methylcitrate synthase has been found in the genome of *S. erythraea*. There are at least six genetic loci encoding putative biotin-dependent acetyl-CoA/propionyl-CoA carboxylases, including SACE_0026–0028, SACE_3241–3242, SACE_3398–3400, SACE_7038–7039, SACE_4237, and SACE_3856/6509–6510 (17). Here, we show that only the genetic locus SACE_3398–3400 (herein named *pccB*, *pccC*, and *pccA*) plays an important role in propionyl-CoA assimilation when *n*-propanol is added for high production of erythromycin. The TetR family transcriptional regulator SACE_3396 (herein named PccD) can bind directly to the promoter regions of *pccBC* and *pccA* and negatively regulate their transcription.

RESULTS

The *pccBC* and *pccA* operons are induced by propanol and propionate in *S. erythraea*. It was reported that propionyl-CoA carboxylases were upregulated when propanol or propionate was added to microorganisms (18, 19). Propanol is converted into propionate, which is subsequently metabolized to propionyl-phosphate or propionyl-CoA by propionate kinase or acetyl/propionyl-CoA synthetase (Fig. 1A). The quantitative analysis of metabolic carbon flux indicated that a high consumption rate of propanol increased intracellular concentration of propionyl-CoA and methylmalonyl-CoA (11) to enhance the biosynthesis of erythromycin. In the genome of *S. erythraea*, loci for at least six possible acetyl-CoA/propionyl-CoA carboxylases are annotated, namely, SACE_0026–0028, SACE_3241–3242, SACE_3398–3400, SACE_7038–7039, SACE_4237, and SACE_6509 (see Fig. S1 in the supplemental material). The cotranscription of genes in each locus was investigated (see Fig. S2 in the supplemental material). We found that gene *pccB* (SACE_3398) was cotranscribed with *pccC* (SACE_3399), forming the *pccBC* operon, and was not cotranscribed with *pccA*

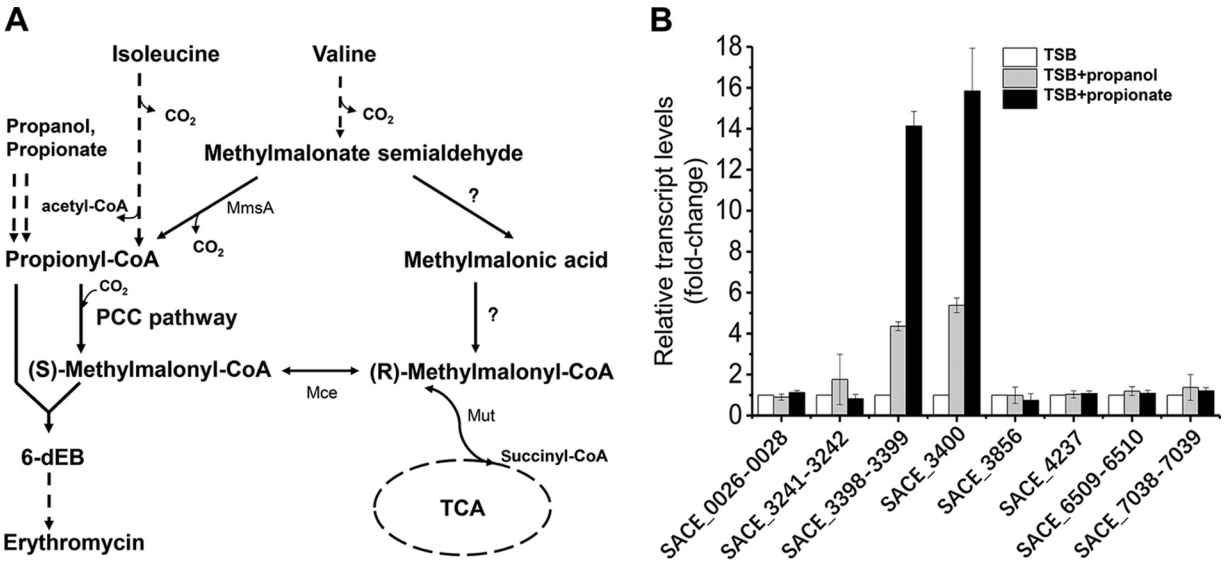

FIG 1 *pccBC* (SACE_3398–3399) and *pccA* (SACE_3400) operons are induced by propanol and propionate in *S. erythraea*. (A) In *S. erythraea*, branched-chain amino acids (BCAA) are a source of propionyl-CoA and methylmalonyl-CoA, key precursors in erythromycin biosynthesis. Valine and isoleucine were metabolized to propionyl-CoA through the degradation pathways. Propanol and propionate are two important external sources of propionyl-CoA, especially in the production of erythromycin. The metabolism of propionyl-CoA to (2*S*)-methylmalonyl–CoA is via the PCC pathway in *S. erythraea*, which plays an important role in propionyl-CoA assimilation when *n*-propanol or valine is added for high production of erythromycin. Enzymes that transform methylmalonate-semialdehyde to (*R*)-methylmalonyl–CoA (indicated by question marks) have not yet been investigated in *S. erythraea*. (B) Total RNA of *S. erythraea* NRRL2338 was extracted after 36 h of growth (see Fig. S3 in the supplemental material) in TSB medium, TSB supplied with 1% (vol/vol) *n*-propanol, and TSB supplied with 20 mM propionate. Relative transcript levels were normalized to the 16S rRNA. The transcription value of each gene in *S. erythraea* in TSB medium was arbitrarily normalized to 1. Error bars represent the standard deviations from three biological replicates. MmsA, methylmalonate-semialdehyde dehydrogenase (acylating); Mut, methylmalonyl-CoA mutase; Mce, methylmalonyl-CoA epimerase.

(SACE_3400). So far, it is still unclear which of the possible propionyl-CoA carboxylases make a contribution to erythromycin biosynthesis. To investigate which genetic loci were responsive to the addition of *n*-propanol or propionate, transcript levels of all loci encoding acetyl-CoA/propionyl-CoA carboxylases were examined using reverse transcription-quantitative PCR (qRT-PCR) (Fig. 1B). The results showed that transcriptional levels of the *pccBC* operon and *pccA* gene increased 4- or 14-fold and 5- or 16-fold, respectively, by addition of propanol or propionate. No changes were observed in transcriptional levels of the other loci coding for acetyl-CoA/propionyl-CoA carboxylases (Fig. 1B). *pccB* encodes a β-subunit (PccB) that has a carboxyl transferase (CT) activity, and *pccA* codes for a larger α-subunit (PccA) comprising the biotin carboxylase (BC) and biotin carboxy carrier protein (BCCP). *pccC* encodes the small ε-subunit (17). These results indicate that *pccBC* and *pccA* operons perform a major function in propionate metabolism and propionyl-CoA assimilation.

PccD (SACE_3396) binds to the promoter regions of *pccBC* and *pccA* operons. To identify the possible transcriptional regulator controlling *pccBC* and *pccA* in *S. erythraea*, we analyzed their genomic organization. It was found that the SACE_3396 gene encoding a TetR/AcrR family transcriptional regulator (named PccD) was located upstream of *pccBC* (Fig. 2A). To examine the binding activity of PccD to *pccBC* and *pccA* operons, electrophoretic mobility shift assays (EMSA) were performed. As shown in Fig. 2B, obvious band shifts were observed, as the entire promoter regions of *pccBC* and *pccA* were incubated with purified recombinant His-tagged PccD (fractions G, H and I) (see Fig. S4 in the supplemental material). The results indicate that PccD was able to directly interact with the promoter regions of these two operons.

PccD is a transcriptional repressor of *pccBC* and *pccA* operons. To further investigate the regulatory effect of PccD on *pccBC* and *pccA* operons, we constructed a *pccD*-deleted mutant (Δ*pccD*) and a *pccD*-overexpressed strain (WT/PIB-*pccD*) and performed transcriptional analysis by qRT-PCR of wild-type (WT), Δ*pccD* and WT/PIB-

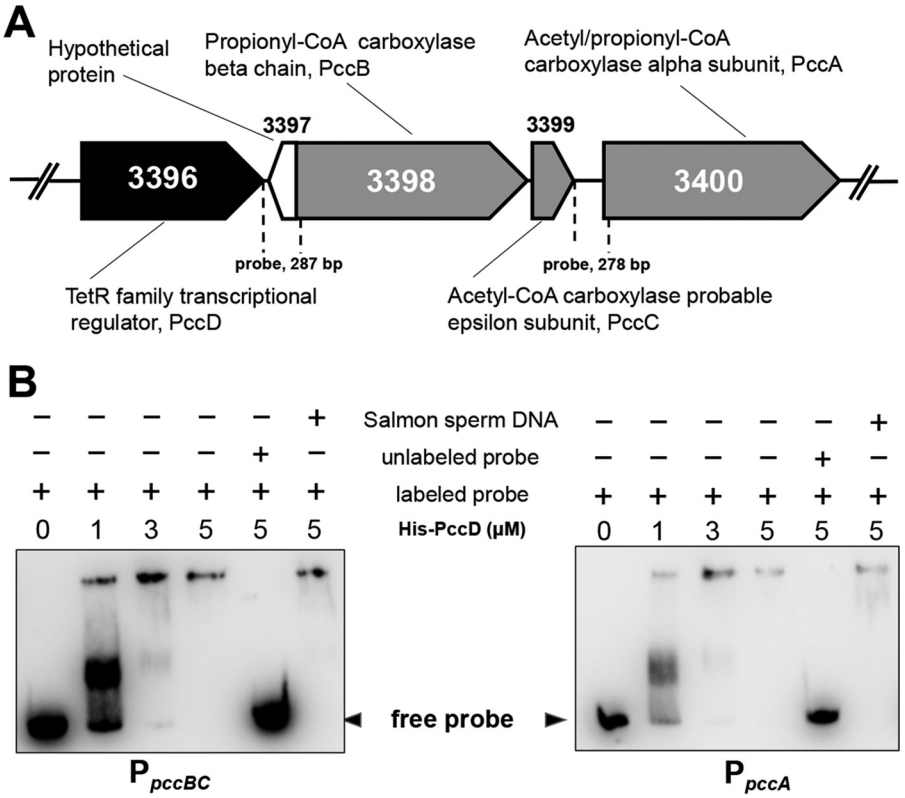

FIG 2 PccD (SACE_3396) binds to the promoter regions of *pccBC* and *pccA*. (A) Genetic organization of the *pccD* gene in the *S. erythraea* genome. *pccB* (SACE_3398), *pccC* (SACE_3399), and *pccA* (SACE_3400) encode a propionyl-CoA carboxylase β-chain, acetyl-CoA carboxylase probable ε-subunit, and acetyl/propionyl-CoA carboxylase α-subunit, respectively. The numbers between dashed lines show the lengths of the promoter regions of *pccBC* and *pccA*, respectively, used in the gel shift experiment shown in panel B. (B) EMSA of His-PccD protein with promoter regions (separated by dashed lines shown in panel A) of *pccBC* or *pccA*. The biotin-labeled DNA probe (about 15 ng, reaction system 10 μl) was incubated with a protein concentration gradient (0, 1, 3, and 5 μM). An unlabeled specific probe (200-fold) or nonspecific competitor DNA (200-fold, sonicated salmon sperm DNA) was used as control. The free probes that did not bind with protein are shown by arrowheads.

pccD strains. These strains were cultivated in tryptone soya broth (TSB) medium, and RNA was extracted at the late exponential growth/early stationary phase. Results show that deletion of *pccD* resulted in a 15-fold (for *pccA*) and 37-fold (for *pccBC*) upregulation of the *pccA* and *pccBC* operons, and that overexpression (approximately 5-fold) of *pccD* inhibited the expression of two operons by 3-fold compared to that in the WT strain (Fig. 3A). Next, we examined the growth of WT, Δ*pccD*, and WT/PIB-*pccD* strains cultivated in Evans media with 20 mM sodium propionate as the sole carbon source. As shown in Fig. 3B, differences in growth behavior were observed among these strains. On one hand, the deletion of *pccD* significantly promoted propionate metabolism and propionyl-CoA assimilation by inducing the transcription of *pccBC* and *pccA* operons, and increased the growth rate of *S. erythraea* on propionate medium (see Fig. S5 in the supplemental material). On the other hand, the WT/PIB-*pccD* strain overexpressing *pccD* revealed a decrease in growth rate on propionate compared to the wild-type strain due to the low levels of *pccBCA* transcripts (Fig. 3A). Meanwhile, the WT/PIB-*pccD* strain showed a decrease in growth yield probably due to the accumulation of toxic propionyl-CoA (12–16). Three strains revealed similar growth curves on Evans media supplied with 2.5% glucose (Fig. 3C). Taken together, these observations further demonstrate that PccD is a transcriptional repressor of *pccBC* and *pccA* operons, and inhibits propionyl-CoA assimilation.

Identification of the PccD-binding sites in upstream regions of *pccBC* and *pccA*. To define the binding sites of PccD, the upstream region (300 bp) of *pccBC* bound by

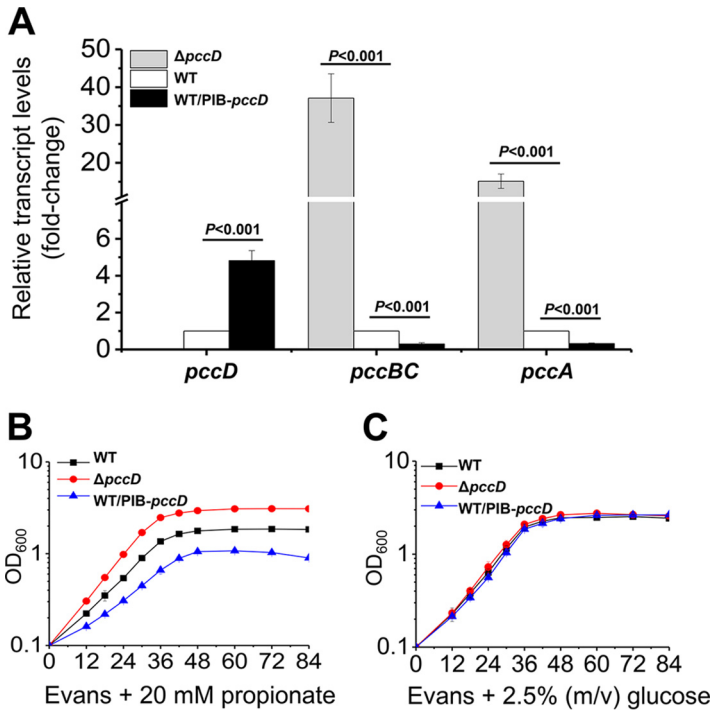

FIG 3 PccD is a repressor of *pccBC* and *pccA* operons. (A) qPCR analysis of the relative transcription levels of *pccD*, *pccBC*, and *pccA* genes between the WT, Δ*pccD*, and WT/PIB-*pccD* strains. Total RNA of these strains was extracted after 36 h of growth in TSB medium (see Fig. S5A in the supplemental material). The expression levels of genes in the WT strain were arbitrarily set to 1.0. Error bars indicate standard deviation from three independent experiments. (B and C) Growth curves of *S. erythraea* strains WT, Δ*pccD*, and WT/PIB-*pccD* grown on Evans medium supplemented with 20 mM sodium propionate (B) or 2.5% glucose (C) as the sole carbon source. Error bars indicate standard deviation from three biological replicates.

recombinant His-tagged PccD was investigated by DNase I footprint mapping. As shown in Fig. 4A, a protected region of 27 nucleotides was detected at the position −140 to −114 relative to the translational start site in the *pccBC* promoter. The −35 promoter sequence (predicted by the Softberry web tool) was located in the protected region (Fig. 4B). A putative PccD-binding motif (t/aTGACGg/cTGt/cTGt/a) was obtained from the protected sequence and the promoter sequence of *pccA* using MEME (http://meme-suite.org/) (Fig. 4C). To further confirm the putative PccD-binding motif, two short biotin-labeled double-stranded DNA (dsDNA) fragments, named M-*pccBC* and M-*pccA* (containing PccD-binding sequences in the upstream regions of *pccBC* and *pccA* operons, respectively) were synthesized (see Table S1 in the supplemental material) and incubated with purified recombinant His-tagged PccD. The EMSA results showed that the two synthetic fragments containing the PccD-binding motif were sufficient to interact with the His-tagged PccD (Fig. 4D), thus confirming the PccD-binding motif predicted by DNase I footprint mapping and MEME method. No PccD-binding motif was observed in the promoter region of *pccD* gene. Indeed, EMSA experimental results revealed that PccD did not bind to its own gene promoter (data not shown).

The metabolite methylmalonic acid is an effector of PccD. TetR/AcrR family transcriptional repressors are homodimeric DNA-binding proteins. Their DNA-binding activity is allosterically inactivated by the binding of small-molecule ligands (effectors). PccD protein from *S. erythraea* contains two TetR domains and may act as a monomer for DNA-binding. To identify the effector of PccD, we investigated several intermediate metabolites of the propionate metabolism as effector molecules, including propionyl-CoA, methylmalonic acid, methylmalonyl-CoA, and succinyl-CoA, as well as propionate itself. The effect of these compounds on PccD binding to the *pccBC* promoters was examined using the EMSA. We found that propionate, propionyl-CoA, methylmalonyl-

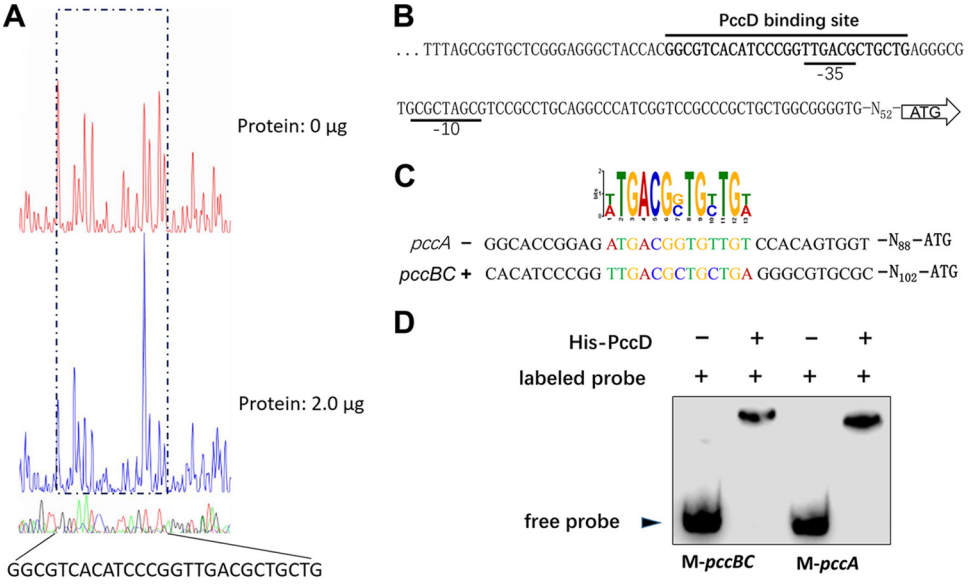

FIG 4 Identification of a PccD-binding site in *pccBC* and *pccA* operons. (A) Electropherograms of a DNase I digest of *pccBC* promoter probe incubated without (top) or with (bottom) 2.0 μg of His-PccD. The nucleotide sequence protected by His-PccD is indicated below. (B) Protected sequence stretches in the upstream regions of *pccBC*. Black lines indicate the regions of DNase I protection. The −35 and −10 sites were predicted by the Softberry web tool. (C) Analysis of the PccD-binding motif of *pccA* using MEME. The standard code of the WebLogo server is shown at the top. (D) Verification of PccD-binding motif by EMSA. Synthetic probes M-*pccBC* and M-*pccA* containing PccD-binding site in promoters of *pccBC* and *pccA* operons, respectively. The DNA probe was incubated with a protein concentration of 5 μM.

CoA, and succinyl-CoA had no effect on the DNA-binding activity of PccD, whereas methylmalonic acid specifically inhibited PccD binding to the *pccBC* promoter (Fig. 5A). In order to further verify the important effect of methylmalonic acid on *pccBC* operon transcription *in vivo* in *S. erythraea*, 10 mM methylmalonic acid was added to TSB medium and the transcriptional level of *pccBC* operon was investigated. The results showed that the *pccBC* operon transcriptional level was increased about more than 26-fold by addition of methylmalonic acid (Fig. 5B). This indicated that methylmalonic acid may exert an important effect on the transcription of the *pccBC* operon, although

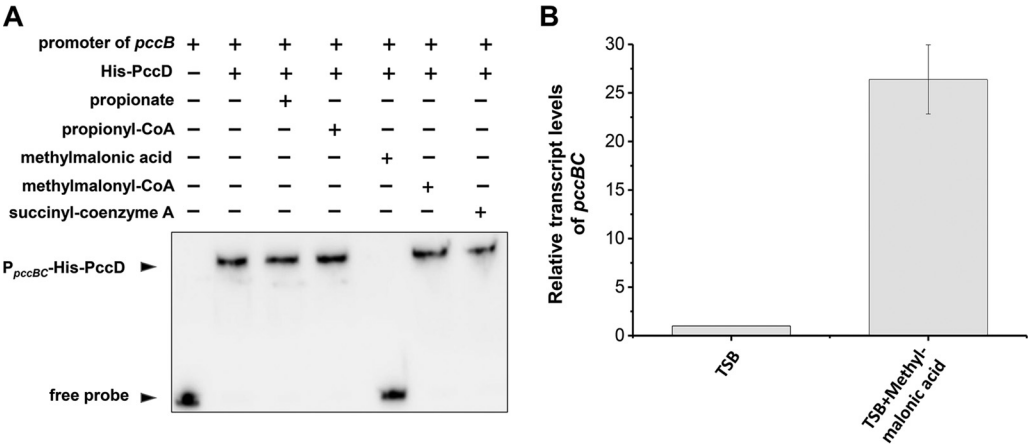

FIG 5 The metabolite methylmalonic acid is an inhibitor of PccD. (A) EMSA of His-PccD protein binding to the upstream promoter regions of *pccBC*. The biotin-labeled DNA probe (about 15 ng, reaction system 10 μl) was incubated with 5 μM His-PccD. Propionate, propionyl-CoA, methylmalonic acid, methylmalonyl-CoA, or succinyl-CoA was added as a cofactor to a final concentration of 1.0 mM. (B) Total RNA of *S. erythraea* NRRL2338 was extracted after 36 h of growth in TSB medium or TSB supplied with 10 mM methylmalonic acid. Relative transcript levels were normalized to the 16S rRNA. The transcription value of *pccBC* in *S. erythraea* WT cultivated in TSB medium was arbitrarily normalized to 1. Error bars represent the standard deviations from three biological replicates.

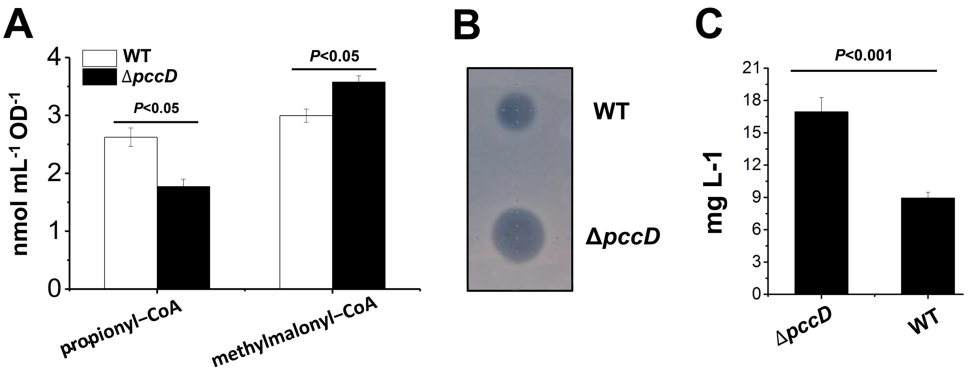

FIG 6 Apparent increase of erythromycin production in the *pccD* deletion strain compared to wild type. (A) Intracellular propionyl-CoA and methylmalonyl-CoA concentration of *S. erythraea* WT and Δ*pccD* strains grown in TSB medium with 1% (vol/vol) *n*-propanol. Cells were harvested at 36 h (see Fig. S5B in the supplemental material). (B) Inhibition tests of *S. erythraea* WT and Δ*pccD* fermentation broths, collected after culturing for 84 h, against *Bacillus subtilis*. (C) Erythromycin concentration of *S. erythraea* WT and Δ*pccD* strains grown in TSB medium with 1% (vol/vol) *n*-propanol. Supernatants were collected after culture for 84 h. A turbidimetric method for microbiological assay of antibiotics was used to quantify the erythromycin levels as described in Materials and Methods. Three independent experiments were performed to calculate standard deviation.

there is no direct experimental evidence that methylmalonic acid is an effector of PccD regulator *in vivo* in *S. erythraea*.

Δ*pccD* probably promotes erythromycin production by activating propionyl-CoA assimilation. From the results described above, we speculated that enhancement of the propionyl-CoA carboxylation might result in an increase of intracellular methylmalonyl-CoA and promote erythromycin production. To verify this speculation, we determined the intracellular concentration of propionyl-CoA and methylmalonyl-CoA in WT and Δ*pccD* strains grown on TSB medium with 1% (vol/vol) *n*-propanol. As shown in Fig. 6A, the result demonstrated that deletion of *pccD* promoted propionyl-CoA carboxylation, resulting in a decrease in propionyl-CoA concentration and an increase in methylmalonyl-CoA concentration. It is known that the biosynthesis of a unit erythromycin needs one propionyl-CoA and six (2*S*)-methylmalonyl–CoAs. A high ratio of methylmalonyl-CoA/propionyl-CoA in the Δ*pccD* strain will facilitate the biosynthesis of erythromycin. Indeed, the Δ*pccD* strain revealed a higher erythromycin yield than the WT strain (Fig. 6B and C).

DISCUSSION

Common and distinctive features of propionyl-CoA assimilation in actinobacteria. Propionyl-CoA is generated from the β-oxidation of odd-chain fatty acids and branched-chain fatty acids, as well as branched-chain amino acids and cholesterol. Propionyl-CoA is toxic if accumulated inside the cell, and thus propionyl-CoA metabolism needs to be tightly regulated to prevent its accumulation and alleviate toxicity (12–16). In most microorganisms, propionyl-CoA levels are controlled via at least two known metabolic pathways: MCC and the PCC/methylmalonyl-CoA pathway. Propionyl-CoA assimilation and metabolism have been investigated only in a few actinobacteria, such as *Mycobacterium tuberculosis* and *Corynebacterium glutamicum* (20–23). Previous studies showed that *M. tuberculosis* contains both pathways of propionyl-CoA assimilation (24, 25). It was found that *S. erythraea* has no MCC for propionyl-CoA assimilation. Genome sequence analysis suggests that the PCC pathway plays a role in propionyl-CoA assimilation in *S. erythraea*. Six genetic loci may encode biotin-dependent carboxylases that catalyze the carboxylation of propionyl-CoA to methylmalonyl-CoA for biosynthesis of erythromycin.

The transcriptional control of gene expression involved in propionyl-CoA assimilation has been investigated in *C. glutamicum* and *M. tuberculosis*. In *M. tuberculosis*, the transcriptional regulator LrpG (also known as PrpR and Rv1129c) controls the expression of genes encoding enzymes of the MCC pathway (24, 26, 27). In *C. glutamicum*, the

PrpR regulator activates the *prpDBC2* operon encoding the enzymes 2-methylcitrate dehydratase (PrpD2), 2-methylisocitrate lyase (PrpB2), and 2-methylcitrate synthase (PrpC2); 2-methylcitrate probably acts as coactivator of PrpR (23, 28). The transcriptional regulation of the genes encoding enzymes of the PCC pathway in bacteria remains unknown. Recently, Carter and Alber found that RSP_2186 (designated PccR) controls the transcription of the propionyl-CoA carboxylase gene in *Rhodobacter sphaeroides* (19). They defined a novel family of short-chain fatty acyl-CoA regulators (ScfRs) that modulate pathways for short-chain acyl-CoA assimilation in microorganisms, including PccR (PCC pathway for propionyl-CoA assimilation), MccR (MCC for propionyl-CoA assimilation), RamB (glyoxylate bypass for acetyl-CoA assimilation), and IbcR (for isobutyryl-CoA assimilation) (19). ScfRs typically belong to the xenobiotic response element (XRE) family and have a helix-turn-helix N-terminal domain for DNA binding and a C-terminal domain of unknown function (DUF2083) as common features. In this study, we found that the TetR/AcrR family transcriptional regulator PccD negatively controlled propionyl-CoA assimilation. *S. erythraea* PccD is a novel ScfR, as it does not belong to the XRE family regulator described by Carter and Alber (19).

BldD, a key developmental regulator in actinobacteria, was identified as directly activating the transcription of all genes involved in the biosynthesis of erythromycin (29). More recently, it was found that two TetR family regulators (SACE_7301 and SACE_3986) were associated with biosynthesis of erythromycin in *S. erythraea* A226. SACE_7301 activated the transcription of the erythromycin biosynthetic gene *eryAI* and the resistance gene *ermE* by interacting with their promoter regions (30). SACE_3986 negatively controlled erythromycin biosynthesis by reducing the transcription of its adjacent gene SACE_3985, which codes for a short-chain dehydrogenase/reductase (31). Herein, PccD, a TetR family regulator, was found to negatively regulate erythromycin biosynthesis by repressing feeder pathways.

The important role of propionyl-CoA carboxylation for high production of erythromycin with *n*-propanol supplementation. In *S. erythraea*, branched-chain amino acids (BCAA) are a source of propionyl-CoA and methylmalonyl-CoA, key precursors in erythromycin biosynthesis. As shown in Fig. 1A, two degradation pathways of valine may exist for the generation of methylmalonyl-CoA from valine: the MPMS (Val→methylmalonate-semialdehyde→propionyl-CoA→methylmalonyl-CoA→succinyl-CoA) pathway and the predicted MMMS (Val→methylmalonate-semialdehyde→methylmalonate→methylmalonyl-CoA→succinyl-CoA) pathway (32, 33). Methylmalonyl-CoA is a limiting factor for erythromycin biosynthesis. In actinobacteria, at least four pathways have been found to generate methylmalonyl-CoA: (i) the PCC pathway for carboxylation of propionyl-CoA by propionyl-CoA carboxylase, (ii) the methylmalonyl-CoA mutase (MCM) pathway that catalyzes the reversible isomerization of succinyl-CoA and methylmalonyl-CoA by methylmalonyl-CoA mutase, (iii) the CCR pathway through crotonyl-CoA reductase or isobutyryl-CoA mutase, and (iv) the meaA pathway from acetoacetyl-CoA (8, 17). No CCR or meaA pathway is found in *S. erythraea*, whereas the PCC and MCM pathways play important roles in the precursor supply under different conditions (6–8, 17). Reeves et al. have proposed a metabolic model in which, in carbohydrate-based fermentations, MCM acts as a drain on the methylmalonyl-CoA metabolite pool; in oil-based fermentations, MCM acts in the reverse direction to fill the methylmalonyl-CoA pool (7). Engineering of the methylmalonyl-CoA metabolic flux of *S. erythraea* through duplication of the methylmalonyl-CoA mutase operon resulted in a 50% increase in erythromycin production in an oil-based fermentation medium (7). Under industrial medium conditions, the increase in methylmalonyl-CoA pool is mainly attributed to the PCC pathway from propionyl-CoA. Some genes involved in the branched-chain amino acid degradation pathway, such as *ilvB* (SACE_4565), *acd* (SACE_4125 and SACE_5025), and *mmsA* (SACE_4672), are significantly upregulated in industrial highly producing strains. These results indicate that propionyl-CoA can be derived from valine, leucine, and isoleucine degradation (9). The addition of *n*-propanol to the medium significantly increases the propionyl-CoA pool as a result of propionate metabolism by acetyl/propionyl-CoA synthetases. There-

TABLE 1 Bacterial strains and plasmids used in this work

Strain or plasmid	Characteristic(s)	Source or reference
Strains		
S. erythraea NRRL2338	Used as parental strain, wild type	DSM 40517
Δ*pccD* strain	*S. erythraea pccD* null mutant, thiostrepton resistance	This work
WT/PIB-*pccD*	*pccD* overexpression strain, WT carrying pIB-*pccD*	This work
E. coli Rosetta (DE3)	F^- *ompT* $hsdS_B(r_B^-\ m_B^-)$ *gal dcm* λ(DE3)pRARE²(Cam^r)	Novagen
Plasmids		
pET19b	Expression vector, Amp^r	Novagen
pET-*pccD*	pET19b derivative carrying *pccD*	This work
pMD-18T	TA-cloning vector	TaKaRa
pUC19-tsr	pUC18 derivative containing a 1.36-kb fragment of a thiostrepton resistance cassette in the BamHI/SmaI sites	34
pUC-*pccD*	pUC19-tsr, with the 1.5-kb DNA fragments upstream and downstream of *pccD* gene inserted upstream and downstream of tsr correspondingly	This work
pIB139	*E. coli-S. erythraea* integrative shuttle vector containing a strong constitutive *ermE** promoter, apramycin resistance	35
pIB-*pccD*	pIB139 carrying an extra *pccD* for the gene overexpression	This work

fore, PccD-regulated PCC-pathway for propionyl-CoA carboxylation plays an important role in high erythromycin production.

In conclusion, short-chain acyl-CoAs are intermediates and precursors for the biosynthesis of many antibiotics. The regulation of their supplies is crucial for increasing antibiotic yield. Our work has identified the novel regulator PccD that controls the gene expression of propionyl-CoA carboxylase, which is responsible for propionyl-CoA assimilation in *S. erythraea*. PccD represses the generation of methylmalonyl-CoA through carboxylation of propionyl-CoA and reveals an effect on biosynthesis of erythromycin. A higher level of erythromycin in the Δ*pccD* strain was observed compared with that in the wild-type strain. Our study reveals a regulatory mechanism in propionate metabolism and suggests new possibilities for designing metabolic engineering to increase erythromycin yield.

MATERIALS AND METHODS

Bacterial strains, plasmids, and growth conditions. Bacterial strains and plasmids used in this study are listed in Table 1. *S. erythraea* NRRL2338 was grown on R2YE agar plates for 5 to 6 days at 30°C for sporulation. An agar piece of about 1 cm^2 was inoculated into a 150-ml flask containing 30 ml of tryptone soya broth (TSB) medium and grown at 30°C and 200 rpm for 48 h for seed stock preparation. Prior to inoculation, the seed was centrifuged at 2,880 × *g* for 10 min at 4°C to form a pellet and then resuspended and washed three times with the next corresponding medium. Next, about 0.5 to 1 ml of the seed culture was added to a 500-ml flask containing 50 ml TSB (initial optical density at 600 nm [OD_{600}] = 0.05) or minimal Evans medium (36) (initial OD_{600} = 0.1) supplemented with various carbon sources grown at 30°C and 200 rpm for genomic DNA extraction, phenotype, or transcription studies.

RNA preparation and qRT-PCR. *S. erythraea* wild-type (WT), *pccD* gene deletion (Δ*pccD*), and *pccD* overexpression (WT/PIB-*pccD*) strains were grown to late-exponential growth/early stationary phase at 30°C in TSB liquid media or TSB supplemented with 1% (vol/vol) propanol, 20 mM propionate, or 10 mM methylmalonic acid. The cells were harvested at 36 h by centrifugation at 4°C, 1,500 × *g* for 10 min. Total RNA was prepared using the RNAprep pure cell/bacteria kit (Tiangen Biotech, Beijing, China). RNA integrity was analyzed by 1% agarose gel electrophoresis. RNA concentration was quantitated by SynergyMx multimode microplate reader (BioTek, Winooski, VT). DNase digestion was performed to remove genomic DNA before reverse transcription for 5 min at 42°C. Total RNA (1 μg) was reverse transcribed using the PrimeScript RT reagent kit (TaKaRa, Kusatsu, Japan). Quantitative PCR (qPCR) was conducted using the SYBR Premix *Ex Taq* GC kit (TaKaRa, Japan), and about 50 ng cDNA was added to a final PCR volume of 20 μl. PCR was performed using the primers (see Table S1 in the supplemental material) with a final concentration of 0.25 μM. PCR assays were carried out using a CFX96 real-time system (Bio-Rad, CA) with the thermocycling conditions as follows: 95°C for 5 min, followed by 40 cycles of 95°C for 10 s, 60°C for 10 s, and 72°C for 30 s, with a final extension cycle at 72°C for 10 min. 16S_rRNA is used as the reference gene. qRT-PCR validation information on amplification efficiency, calibration curves with slope and R^2, and specificity (melt) are shown in Data Set S1 in the supplemental material. Data analyses of qRT-PCR are shown in Data Sets S2 to S4 in the supplemental material. STDEV indicates the standard deviation derived from three independent experiments.

Protein overexpression and purification. To produce the PccD protein, the *pccD* gene was amplified from *S. erythraea* NRRL2338 by PCR using *pccD*-F/-R primers (Table S1) and cloned into pET-19b, generating the recombinant plasmid pET-*pccD* (Table 1). The correct gene sequences were confirmed by

sequencing analysis and the recombinant plasmids were introduced into *Escherichia coli* Rosetta (DE3) competent cells. The recombinant cells selected by ampicillin were grown in 5 ml LB medium with 100 mg liter^{-1} ampicillin in an orbital shaker (200 rpm, 37°C) for 12 h. Next, 2.5 ml of the seed culture was added to a 250-ml flask containing 50 ml terrific broth (TB) medium (24 g liter^{-1} yeast extract, 12 g · liter^{-1} tryptone, 0.4% glycerol, 17 mM KH_2PO_4, and 72 mM K_2HPO_4) followed by incubation at 20°C for 20–24 h. His_6-tagged PccD protein (His-PccD) was purified from Rosetta (DE3)-harboring pET-*pccD* as previously described (37). Purity of the purified protein was checked by SDS-PAGE (Fig. S4). The fractions G, H, and I were pooled and used in the assay. The protein concentration was determined using the Bradford assay.

Electrophoretic mobility shift assay. The putative promoter regions of the target genes were amplified by PCR using the primers listed in Table S1. PCR products were labeled with biotin using a universal biotinylated primer (5′biotin-AGCCAGTGGCGATAAG-3′). The biotin-labeled PCR products were purified using the PCR purification kit (Shanghai Generay Biotech, China) as electrophoretic mobility shift assay (EMSA) probes. EMSAs were carried out using a chemiluminescent EMSA kit (Beyotime Biotechnology, China), as previously described (37). Biotin-labeled DNA probes were incubated with a gradient concentration of proteins at 25°C for 20 min. For control groups, an unlabeled specific probe (200-fold) or nonspecific competitor DNA (200-fold, sonicated salmon sperm DNA) was used. Samples were separated by 6% nondenaturing PAGE gels in ice-cold 0.5× Tris-borate-EDTA at 160 V, and bands were detected by BeyoECL Plus (Beyotime Biotechnology, China).

To verify the conserved PccD-binding motif, two short biotin-labeled dsDNA probe named M-*pccBC* and M-*pccA*, containing PccD-binding site in the promoters of *pccBC* and *pccA* operons, respectively, were synthesized (Table S1) and incubated with purified recombinant His-tagged PccD. In EMSA, an excess of poly[d(I-C)] was added during incubation to avoid nonspecific binding of the protein to the DNA.

Construction of the *pccD* in-frame deletion mutant and overexpression strain. For an insertional deletion of the *pccD* gene, a previously described homologous recombination strategy was used (34). 1.5-kb DNA fragments upstream and downstream of the *pccD* gene locus were amplified from *S. erythraea* NRRL2338 genomic DNA by PCR using the primer pair pUC3396upF/R, pUC3396dwF/R (Table S1). The PCR products were digested with HindIII/XbaI and KpnI/EcoRI and subsequently inserted into the corresponding sites of pUC19-tsr, creating pUC-*pccD* knockout plasmids (Table 1). The thiostrepton-resistance cassette amplified from pUC-*pccD* knockout plasmids by PCR using the primer pair pUC3396upF/pUC3396dwR was transferred into *S. erythraea* by polyethylene glycol (PEG)-mediated transformation. The mutants were selected by thiostrepton on R_3M agar plates. The selected mutants were verified by PCR and DNA sequencing (see Fig. S6 in the supplemental material). Primers are listed in Table S1.

For overexpression of the mutants, the *pccD* gene was PCR-amplified with the primer pair 3396over-F/R (Table S1). The PCR products were then cloned into NdeI/NotI sites of pIB139, creating the pIB-*pccD* plasmid (Table 1). The overexpression plasmids were introduced into the *pccD* mutant strain (SeryΔ*pccD*) by PEG-mediated transformation. The desired overexpression strains were screened by apramycin resistance and confirmed by PCR.

Erythromycin assay. A turbidimetric method for microbiological assay of antibiotics was used to quantify the erythromycin levels as previously described (38), with modifications. Briefly, the supernatant (cultivated in TSB with 1% [vol/vol] *n*-propanol) was collected after culture for 84 h of the *S. erythraea* wild-type (WT), *pccD* deficient strain (Δ*pccD*) and diluted by 40 times before use as test samples. *Staphylococcus aureus* was cultivated on medium (peptone, 6 g; pancreatic digest of casein, 4 g; beef extract, 1.5 g; yeast extract, 3 g; glucose monohydrate, 1 g; and agar, 15 g; per 1,000 ml water) for 16 to 18 h at 37°C for use as the sensitive microorganism. 15 μl erythromycin standard (0.1 μg to 0.8 μg) or test sample was added to a 96-well plate. 135 μl medium (peptone, 6 g; beef extract, 1.5 g; yeast extract, 3 g; sodium chloride, 3.5 g; glucose monohydrate, 1 g; dipotassium hydrogen phosphate, 3.68 g; potassium dihydrogen phosphate, 1.32 g; per 1,000 ml water) containing a suspension of *Staphylococcus aureus* (to a final OD of 0.05) was added to the wells. Formaldehyde was used as blank to set the optical apparatus. The 96-well plate was placed in a microplate plate incubator at 37°C for 3 to 4 h (OD_{600} was controlled in the range 0.1 to 0.5). The growth of the microorganisms was stopped by adding 7.5 μl of formaldehyde to each well. OD was measured by SynergyMx multimode microplate reader (BioTek, Winooski, VT). Three independent experiments were performed to calculate standard deviation. The bioassay-based erythromycin analysis was also carried out as previously described (30).

Determination of intracellular propionyl-CoA and methylmalonyl-CoA concentrations. For determination of propionyl-CoA and methylmalonyl-CoA concentrations, CoA compound extraction and chromatography were performed as previously described (39). Cells grown for 36 h in TSB medium with 1% (vol/vol) *n*-propanol were harvested by centrifugation, washed twice with phosphate-buffered saline (PBS, pH 8.0), and lysed in lysis buffer (10% trichloroacetic acid and 2 mM dithiothreitol). The cell lysates were frozen and thawed out repeatedly with liquid nitrogen and ice water 2 or 3 times, centrifuged at 4°C, 15,000 × *g*, for 10 min, and transferred to an equilibrated solid-phase extraction column (Sep-Pak, 1 ml, 50 mg tC18; Waters, Milford, MA). After samples were adsorbed, the columns were washed by 0.1% trifluoroacetic acid (TFA) and eluted by 40% acetonitrile with 0.1% TFA. The eluate was dried by SpeedVac (Thermo Fisher, Waltham, MA) and stored at −80°C. For chromatography, the two mobile-phase solvents used were buffer A (75 mM KH_2PO_4, pH 5.5) and buffer B (800 ml of 75 mM KH_2PO_4, pH 5.0, mixed with 200 ml of 20% acetonitrile). The chromatographic separations were performed at room temperature at a flow rate of 0.8 ml/min on an ODS C_{18} column and the samples were monitored at 254 nm. The mobile phase composition profile was divided into several linear gradient segments, with sequential segment endpoints of 10 min (when buffer B reached 28% from 10%), 15 min (buffer B

reached 30% from 28%), 25 min (buffer B 40% reached from 30%), 26 min (buffer B reached 42% from 40%), 35 min (buffer B reached 54% from 42%), and 36 min (buffer B was reduced from 54% to 10%). After a 14-min constant buffer B level of 10%, data collection was stopped at 50 min. Three independent experiments were performed to calculate standard deviation.

DNase I footprinting assay. The promoter region of *pccB* (SACE_3398) was amplified by PCR with primers pMD18T-3398F and -R (Table S1) and the amplicon was cloned into the T-vector pMD-18T (TaKaRa). For preparation of fluorescent 6-carboxyfluorescein (FAM)-labeled probes, the promoter region of *pccB* was PCR-amplified from the obtained plasmids using primers of M13R-48 (FAM) and M13F-47. The FAM-labeled probes were purified using a QIAquick gel extraction kit (Qiagen) and quantified using a NanoDrop 2000C (Thermo Fisher). DNase I footprinting assays were performed as previously described (40). For each assay, 500 ng of probes were incubated with different amounts of His-PccD in a total volume of 40 μl. After incubation for 30 min at 25°C, a 10 μl solution containing about 0.015 unit DNase I (Promega) and 100 nmol freshly prepared $CaCl_2$ was added and further incubated for 1 min at 25°C. The reaction was stopped by adding 140 μl DNase I stop solution (200 mM unbuffered sodium acetate, 30 mM EDTA, and 0.15% SDS). Samples were first extracted with phenol-chloroform and then precipitated with ethanol, and the pellets were dissolved in 30 μl MiniQ water. The preparation of the DNA ladder, electrophoresis, and data analysis were previously described (40), except that the GeneScan-LIZ500 size standard (Applied Biosystems) was used.

SUPPLEMENTAL MATERIAL

Supplemental material for this article may be found at https://doi.org/10.1128/JB.00281-17.

SUPPLEMENTAL FILE 1, PDF file, 0.8 MB.

SUPPLEMENTAL FILE 2, XLSX file, 0.6 MB.

ACKNOWLEDGMENTS

This study was supported by the National Natural Science Foundation of China (grant no. 21575089, 21335003, and 21276079) and the National High-tech R&D Program (863 Program) (grant no. 2014AA021502).

We have no conflict of interest to declare.

REFERENCES

1. Staunton J, Weissman KJ. 2001. Polyketide biosynthesis: a millennium review. Nat Prod Rep 18:380–416. https://doi.org/10.1039/a909079g.
2. Li L, Zhao Y, Ruan L, Yang S, Ge M, Jiang W, Lu Y. 2015. A stepwise increase in pristinamycin II biosynthesis by *Streptomyces pristinaespiralis* through combinatorial metabolic engineering. Metab Eng 29:12–25. https://doi.org/10.1016/j.ymben.2015.02.001.
3. Wang W, Tian J, Li L, Ge M, Zhu H, Zheng G, Huang H, Ruan L, Jiang W, Lu Y. 2015. Identification of two novel regulatory genes involved in pristinamycin biosynthesis and elucidation of the mechanism for AtrA-p-mediated regulation in *Streptomyces pristinaespiralis*. Appl Microbiol Biotechnol 99:7151–7164. https://doi.org/10.1007/s00253-015-6638-6.
4. Zhao Y, Feng R, Zheng G, Tian J, Ruan L, Ge M, Jiang W, Lu Y. 2015. Involvement of the TetR-type regulator PaaR in the regulation of pristinamycin I biosynthesis through an effect on precursor supply in *Streptomyces pristinaespiralis*. J Bacteriol 197:2062–2071. https://doi.org/10.1128/JB.00045-15.
5. Staunton J, Wilkinson B. 1997. Biosynthesis of erythromycin and rapamycin. Chem Rev 97:2611–2630. https://doi.org/10.1021/cr9600316.
6. Reeves AR, Cernota WH, Brikun IA, Wesley RK, Weber JM. 2004. Engineering precursor flow for increased erythromycin production in *Aeromicrobium erythreum*. Metab Eng 6:300–312. https://doi.org/10.1016/j.ymben.2004.03.003.
7. Reeves AR, Brikun IA, Cernota WH, Leach BI, Gonzalez MC, Weber JM. 2007. Engineering of the methylmalonyl-CoA metabolite node of *Saccharopolyspora erythraea* for increased erythromycin production. Metab Eng 9:293–303. https://doi.org/10.1016/j.ymben.2007.02.001.
8. Li YY, Chang X, Yu WB, Li H, Ye ZQ, Yu H, Liu BH, Zhang Y, Zhang SL, Ye BC, Li YX. 2013. Systems perspectives on erythromycin biosynthesis by comparative genomic and transcriptomic analyses of *S. erythraea* E3 and NRRL2338 strains. BMC Genomics 14:523. https://doi.org/10.1186/1471-2164-14-523.
9. Karnicar K, Drobnak I, Petek M, Magdevska V, Horvat J, Vidmar R, Baebler S, Rotter A, Jamnik P, Fujs S, Turk B, Fonovic M, Gruden K, Kosec G, Petkovic H. 2016. Integrated omics approaches provide strategies for rapid erythromycin yield increase in *Saccharopolyspora erythraea*. Microb Cell Fact 15:93. https://doi.org/10.1186/s12934-016-0496-5.
10. El-Enshasy HA, Mohamed NA, Farid MA, El-Diwany AI. 2008. Improvement of erythromycin production by *Saccharopolyspora erythraea* in molasses based medium through cultivation medium optimization. Bioresour Technol 99:4263–4268. https://doi.org/10.1016/j.biortech.2007.08.050.
11. Chen Y, Huang M, Wang Z, Chu J, Zhuang Y, Zhang S. 2013. Controlling the feed rate of glucose and propanol for the enhancement of erythromycin production and exploration of propanol metabolism fate by quantitative metabolic flux analysis. Bioprocess Biosyst Eng 36:1445–1453. https://doi.org/10.1007/s00449-013-0883-9.
12. Brock M, Buckel W. 2004. On the mechanism of action of the antifungal agent propionate. Eur J Biochem 271:3227–3241. https://doi.org/10.1111/j.1432-1033.2004.04255.x.
13. Gregersen N. 1981. The specific inhibition of the pyruvate dehydrogenase complex from pig kidney by propionyl-CoA and isovaleryl-Co-A. Biochem Med 26:20–27. https://doi.org/10.1016/0006-2944(81)90026-0.
14. Maruyama K, Kitamura H. 1985. Mechanisms of growth inhibition by propionate and restoration of the growth by sodium bicarbonate or acetate in *Rhodopseudomonas sphaeroides*. J Biochem 98:819–824. https://doi.org/10.1093/oxfordjournals.jbchem.a135340.
15. Schwab MA, Sauer SW, Okun JG, Nijtmans LG, Rodenburg RJ, van den Heuvel LP, Drose S, Brandt U, Hoffmann GF, Ter Laak H, Kolker S, Smeitink JA. 2006. Secondary mitochondrial dysfunction in propionic aciduria: a pathogenic role for endogenous mitochondrial toxins. Biochem J 398:107–112. https://doi.org/10.1042/BJ20060221.
16. Shaw L, Engel PC. 1985. The suicide inactivation of ox liver short-chain acyl-CoA dehydrogenase by propionyl-CoA. Formation of an FAD adduct. Biochem J 230:723–731.
17. Oliynyk M, Samborskyy M, Lester JB, Mironenko T, Scott N, Dickens S, Haydock SF, Leadlay PF. 2007. Complete genome sequence of the erythromycin-producing bacterium *Saccharopolyspora erythraea* NRRL2338. Nat Biotechnol 25:447–453. https://doi.org/10.1038/nbt1297.
18. Chong PK, Burja AM, Radianingtyas H, Fazeli A, Wright PC. 2007. Pro-

teome analysis of *Sulfolobus solfataricus* P2 propanol metabolism. J Proteome Res 6:1430–1439. https://doi.org/10.1021/pr060575g.
19. Carter MS, Alber BE. 2015. Transcriptional regulation by the short-chain fatty acyl coenzyme A regulator (ScfR) PccR controls propionyl coenzyme A assimilation by *Rhodobacter sphaeroides*. J Bacteriol 197: 3048–3056. https://doi.org/10.1128/JB.00402-15.
20. Upton AM, McKinney JD. 2007. Role of the methylcitrate cycle in propionate metabolism and detoxification in *Mycobacterium smegmatis*. Microbiology 153:3973–3982. https://doi.org/10.1099/mic.0.2007/011726-0.
21. Eoh H, Rhee KY. 2014. Methylcitrate cycle defines the bactericidal essentiality of isocitrate lyase for survival of *Mycobacterium tuberculosis* on fatty acids. Proc Natl Acad Sci U S A 111:4976–4981. https://doi.org/10.1073/pnas.1400390111.
22. Claes WA, Puhler A, Kalinowski J. 2002. Identification of two prpDBC gene clusters in *Corynebacterium glutamicum* and their involvement in propionate degradation via the 2-methylcitrate cycle. J Bacteriol 184: 2728–2739. https://doi.org/10.1128/JB.184.10.2728-2739.2002.
23. Rohde KH, Veiga DF, Caldwell S, Balazsi G, Russell DG. 2012. Linking the transcriptional profiles and the physiological states of *Mycobacterium tuberculosis* during an extended intracellular infection. PLoS Pathog 8:e1002769. https://doi.org/10.1371/journal.ppat.1002769.
24. Griffin JE, Pandey AK, Gilmore SA, Mizrahi V, McKinney JD, Bertozzi CR, Sassetti CM. 2012. Cholesterol catabolism by *Mycobacterium tuberculosis* requires transcriptional and metabolic adaptations. Chem Biol 19: 218–227.
25. Savvi S, Warner DF, Kana BD, McKinney JD, Mizrahi V, Dawes SS. 2008. Functional characterization of a vitamin B12-dependent methylmalonyl pathway in *Mycobacterium tuberculosis*: implications for propionate metabolism during growth on fatty acids. J Bacteriol 190:3886–3895. https://doi.org/10.1128/JB.01767-07.
26. Datta P, Shi L, Bibi N, Balazsi G, Gennaro ML. 2011. Regulation of central metabolism genes of *Mycobacterium tuberculosis* by parallel feed-forward loops controlled by sigma factor E (sigma(E)). J Bacteriol 193: 1154–1160. https://doi.org/10.1128/JB.00459-10.
27. Masiewicz P, Brzostek A, Wolanski M, Dziadek J, Zakrzewska-Czerwinska J. 2012. A novel role of the PrpR as a transcription factor involved in the regulation of methylcitrate pathway in *Mycobacterium tuberculosis*. PLoS One 7:e43651. https://doi.org/10.1371/journal.pone.0043651.
28. Plassmeier J, Persicke M, Puhler A, Sterthoff C, Ruckert C, Kalinowski J. 2012. Molecular characterization of PrpR, the transcriptional activator of propionate catabolism in *Corynebacterium glutamicum*. J Biotechnol 159:1–11. https://doi.org/10.1016/j.jbiotec.2011.09.009.
29. Chng C, Lum AM, Vroom JA, Kao CM. 2008. A key developmental regulator controls the synthesis of the antibiotic erythromycin in *Saccharopolyspora erythraea*. Proc Natl Acad Sci U S A 105:11346–11351. https://doi.org/10.1073/pnas.0803622105.
30. Wu H, Chen M, Mao Y, Li W, Liu J, Huang X, Zhou Y, Ye BC, Zhang L, Weaver DT, Zhang B. 2014. Dissecting and engineering of the TetR family regulator SACE_7301 for enhanced erythromycin production in *Saccharopolyspora erythraea*. Microb Cell Fact 13:158. https://doi.org/10.1186/s12934-014-0158-4.
31. Wu P, Pan H, Zhang C, Wu H, Yuan L, Huang X, Zhou Y, Ye BC, Weaver D, Zhang L, Zhang B. 2014. SACE_3986, a TetR family transcriptional regulator, negatively controls erythromycin biosynthesis in *Saccharopolyspora erythraea*. J Ind Microbiol Biotechnol 41:1159–1167. https://doi.org/10.1007/s10295-014-1449-9.
32. Esser D, Kouril T, Talfournier F, Polkowska J, Schrader T, Brasen C, Siebers B. 2013. Unraveling the function of paralogs of the aldehyde dehydrogenase super family from *Sulfolobus solfataricus*. Extremophiles 17: 205–216. https://doi.org/10.1007/s00792-012-0507-3.
33. Hughes AJ, Keatinge-Clay A. 2011. Enzymatic extender unit generation for in vitro polyketide synthase reactions: structural and functional showcasing of *Streptomyces coelicolor* MatB. Chem Biol 18:165–176. https://doi.org/10.1016/j.chembiol.2010.12.014.
34. Han S, Song P, Ren T, Huang X, Cao C, Zhang B. 2011. Identification of SACE_7040, a member of TetR family related to the morphological differentiation of *Saccharopolyspora erythraea*. Curr Microbiol 63: 121–125. https://doi.org/10.1007/s00284-011-9943-z.
35. Wilkinson CJ, Hughes-Thomas ZA, Martin CJ, Böhm I, Mironenko T, Deacon M, Wheatcroft M, Wirtz G, Staunton J, Leadlay PF. 2002. Increasing the efficiency of heterologous promoters in actinomycetes. J Mol Microbiol Biotechnol 4:417–426.
36. Fink D, Weissschuh N, Reuther J, Wohlleben W, Engels A. 2002. Two transcriptional regulators GlnR and GlnRII are involved in regulation of nitrogen metabolism in *Streptomyces coelicolor* A3(2). Mol Microbiol 46:331–347. https://doi.org/10.1046/j.1365-2958.2002.03150.x.
37. Liao CH, Yao LL, Ye BC. 2014. Three genes encoding citrate synthases in *Saccharopolyspora erythraea* are regulated by the global nutrient-sensing regulators GlnR, DasR, and CRP. Mol Microbiol 94:1065–1084. https://doi.org/10.1111/mmi.12818.
38. Kersey RC, Fink FC. 1954. Microbiological assay of antibiotics, p 53–79. *In* Glick D (ed), Methods of biochemical analysis, vol 1. Interscience Publisher, Inc., New York, NY.
39. Boynton ZL, Bennett GN, Rudolph FB. 1994. Intracellular concentrations of coenzyme A and its derivatives from *Clostridium acetobutylicum* ATCC 824 and their roles in enzyme regulation. Appl Environ Microbiol 60: 39–44.
40. Wang Y, Cen XF, Zhao GP, Wang J. 2012. Characterization of a new GlnR binding box in the promoter of *amtB* in *Streptomyces coelicolor* inferred a PhoP/GlnR competitive binding mechanism for transcriptional regulation of amtB. J Bacteriol 194:5237–5244. https://doi.org/10.1128/JB.00989-12.